

A transport approach to relate asymmetric protein segregation and population growth

Jiseon Min

Department of Molecular and Cellular Biology,
Harvard University, Cambridge, MA 02138, USA

Ariel Amir

E-mail: arielamir@seas.harvard.edu

John A. Paulson School of Engineering and Applied Sciences, Harvard University,
Cambridge, MA 02138, USA

Abstract. Many unicellular organisms allocate their key proteins asymmetrically between the mother and daughter cells, especially in a stressed environment. A recent theoretical model is able to predict when the asymmetry in segregation of key proteins enhances the population fitness, extrapolating the solution at two limits where the segregation is perfectly asymmetric (asymmetry $a = 1$) and when the asymmetry is small ($0 \leq a \ll 1$) [1]. We generalize the model by introducing stochasticity and use a transport equation to obtain a self-consistent equation for the population growth rate and the distribution of the amount of key proteins. We provide two ways of solving the self-consistent equation: numerically by updating the solution for the self-consistent equation iteratively and analytically by expanding moments of the distribution. With these more powerful tools, we can extend the previous model by *Lin et al.* [1] to include stochasticity to the segregation asymmetry. We show the stochastic model is equivalent to the deterministic one with a modified effective asymmetry parameter (a_{eff}). We discuss the biological implication of our models and compare with other theoretical models.

1. Introduction

Genetically identical unicellular organisms may nevertheless exhibit different traits such as growth rate or generation time, a phenomenon known as phenotypic variability [2]. One cause of such diversity is the asymmetric allocation of key proteins at division. For instance, some bacteria and eukaryotic cells accumulate protein aggregates when exposed to stress and tend to segregate more of them to one of the two newborn cells at a division event. As a result, the “rejuvenated” cells (i.e. those with less damage) grow faster than the “senescent” cells [3–8]. There have been a number of theoretical works [1, 9–11] trying to quantify the effect of asymmetric segregation of proteins to the overall growth of the population. In this paper, we strengthen the theory developed by *Lin et al.* [1] to relate the asymmetric protein segregation and the population growth

rate by implementing a more general method involving transport equations and moment expansions. This allows us to recover previous results rigorously, and go beyond them. We extend the model to consider stochastic asymmetric segregation. Lastly, we compare alternative models of asymmetric segregation by applying the self-consistent equations.

2. Model

We define a generalization of the model proposed by *Lin et al.* [1]. Consider a clonal microbial population that grows exponentially with rate Λ_p . We assume that as a cell grows by volume ΔV , the amount of key proteins D increases by $\Delta D = S\Delta V$. Each cell's inter-division time (τ) is a function of the initial concentration of the key protein (σ_b). For simplicity, suppose every cell is born with volume $V_b = 1$ and divides when the volume reaches $V_d = 2$. As it divides, the key proteins segregate asymmetrically according to the asymmetry parameter a : one daughter cell inherits $\frac{1+a}{2}$ of the key proteins from the mother and the other gets the rest. We call the key protein *damaging* if the generation time $\tau[\sigma_b]$ is an increasing function of the initial protein concentration and *beneficial* if it is a decreasing function.

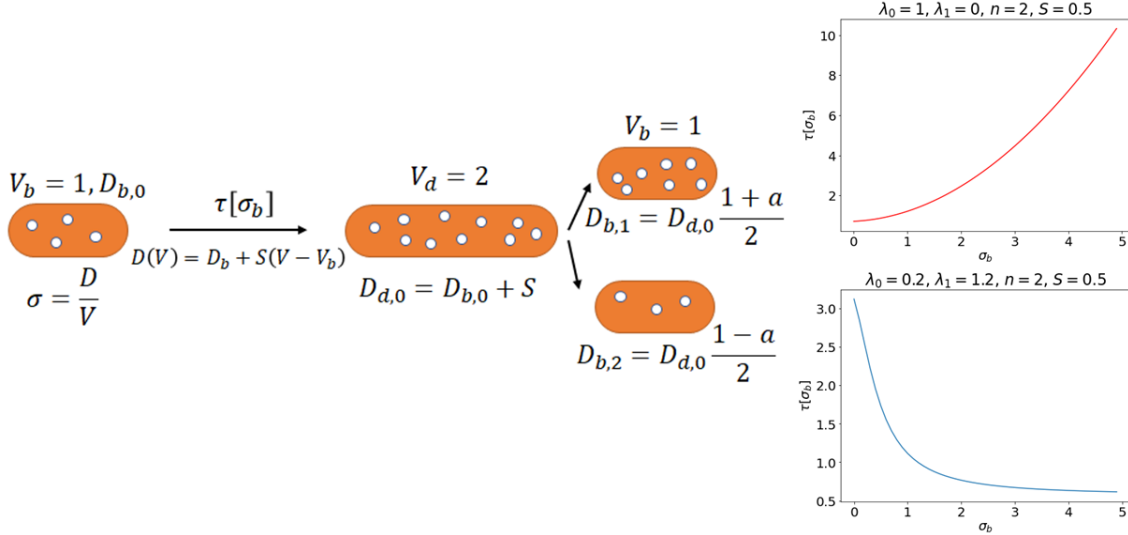


Figure 1: Single cell level model. For simplicity, we assume that every cell has a volume $V_b = 1$ at birth and divides when it reaches $V_d = 2$. The amount of key proteins in a cell increases in proportion to the added volume with a prefactor S . The generation time $\tau[\sigma_b]$ is a function of the key protein concentration at birth ($\sigma_b = D_b/V_b$). Asymmetry $a \in [0, 1]$ tunes the ratio of key proteins inherited by two offspring cells ($a = 0$ being perfectly asymmetric, $a = 1$ being perfectly asymmetric). The plots on the right show an example of generation time as a function of initial concentration of key protein which is detrimental (top) or beneficial (bottom).

While our analysis can be applied to any analytical function $\tau[\sigma_b]$, we assume the instantaneous growth rate is a Hill-type function of the key protein concentration of the

A transport approach to relate asymmetric protein segregation and population growth 3
cell, as proposed by *Lin et al.* [1].

$$\lambda[\sigma] = \frac{\lambda_0 + \lambda_1 \sigma^n}{1 + \sigma^n}, \quad (1)$$

$$\begin{aligned} \tau[\sigma_b] &= \int_1^2 \frac{1}{V\lambda[\sigma]} dV \\ &= \int_1^2 \frac{1}{V\lambda[(\sigma_b - S)/V + S]} dV. \end{aligned} \quad (2)$$

Every time a cell divides, the asymmetry parameter a is randomly and independently drawn from a probability distribution $g(a)$. The deterministic model by *Lin et al.* [1] assumes a delta function for $g(a)$, but here we allow a to fluctuate.

3. Results

3.1. Transport equation

Recently, *Levien et al.* [12] showed that a transport equation can be used to get a self-consistent equation for the population distribution of phenotype and population growth rate even when the properties of the cells are correlated across the generations. Here we follow their derivation by setting the phenotype of interest as the key protein concentration at birth σ_b .

Assume that the population size is N at time t and it grows exponentially with the rate Λ_p . Let us also assume that the population has reached a stable probability distribution $\psi(u, \sigma_b, t)$, where u is time since birth, σ_b is the key protein concentration at birth, and t is the global time. The population then evolves during an infinitesimal time step dt as:

$$\begin{aligned} N\psi(u, \sigma_b, t) &= Ne^{-\Lambda_p dt} \psi(u - dt, \sigma_b, t - dt), \\ &= N(1 - \Lambda_p dt) \left(\psi(u, \sigma_b, t) - dt \frac{\partial \psi}{\partial u} - dt \frac{\partial \psi}{\partial t} \right). \end{aligned} \quad (3)$$

Rearranging the terms and dividing both sides by dt , we get

$$\frac{\partial \psi}{\partial u} + \frac{\partial \psi}{\partial t} = -\Lambda_p \psi. \quad (4)$$

In a steady state population, there is no dependence on t , so $\partial_t \psi = 0$. Therefore,

$$\frac{\partial \psi(u, \sigma_b)}{\partial u} = -\Lambda_p \psi(u, \sigma_b), \quad (5)$$

$$\psi(u, \sigma_b) = \psi(0, \sigma_b) e^{-\Lambda_p u}. \quad (6)$$

The boundary conditions are set by the division. The probability density of having a newborn cell with a protein concentration σ_b is

$$\psi(0, \sigma_b) = 2 \int \int f(\sigma_b | \sigma'_b, a') g(a') \psi(\tau[\sigma'_b], \sigma'_b) d\sigma'_b da'. \quad (7)$$

The probability density $f(\sigma_b|\sigma'_b, a')$ and $g(a')$ depend on the physiological model we choose. For instance, in a deterministic model, we have

$$f(\sigma_b|\sigma'_b, a') = \frac{1}{2}\delta\left(\sigma_b - \frac{1+a'}{2}(\sigma'_b + S)\right) + \frac{1}{2}\delta\left(\sigma_b - \frac{1-a'}{2}(\sigma'_b + S)\right) \quad (8)$$

$$g(a') = \delta(a' - \bar{a}). \quad (9)$$

Applying the solution given by Equation 6 (in the general case), we can eliminate the dependence on u . Thus, we can rewrite to obtain a self-consistent equation:

$$\psi_{\text{birth}}[\sigma_b] = 2 \int \int f(\sigma_b|\sigma'_b, a') \psi_{\text{birth}}[\sigma'_b] g(a') e^{-\Lambda_p \tau[\sigma'_b]} d\sigma'_b da'. \quad (10)$$

In the next section, we apply the self-consistent Equation 10 to a toy model of *E. coli* recently published by *Blitvic et al.* [13] as a simple example.

3.2. Toy model of the aging of *E. coli* [13]

Let us introduce a simple model published by *Blitvic et al.* to demonstrate how to use our approach to connect the asymmetry between two newborn cells and population growth rate [13]. *Blitvic et al.* assume that as an *E. coli* cell divides, one daughter cell is rejuvenated and the other senescent where the generation time of a rejuvenated cell ($\tau[R]$) is shorter than a senescent cell ($\tau[S]$). In this model, there are two phenotype $x = S$ for a senescent cell and $x = R$ for a rejuvenated one.

Then the transition density $f(x|x')$ from a phenotype x' to x is

$$f(x|x') = \frac{1}{2}\delta(x - R) + \frac{1}{2}\delta(x - S). \quad (11)$$

The self-consistent equation is

$$\psi[x] = \int \psi[x'] f(x|x') e^{-\Lambda_p \tau[x']} dx'. \quad (12)$$

Integrating both sides with respect to x , we have

$$1 = e^{-\Lambda_p \tau[R]} + e^{-\Lambda_p \tau[S]}. \quad (13)$$

Because the exponential function is convex, by Jensen's inequality,

$$1 = e^{-\Lambda_p \tau[S]} + e^{-\Lambda_p \tau[R]} > 2e^{-\Lambda_p \langle \tau[x] \rangle}, \quad (14)$$

where $\langle \tau[x] \rangle = \frac{1}{2}(\tau[S] + \tau[R])$. Thus, the asymmetry of generation time of two distinct phenotypes enhances the population growth rate if the mean of the generation time, $\langle \tau[x] \rangle$ is kept constant. Note that Equation 13 was also derived in Ref. [14] in the context of the asymmetric division of the budding yeast *Saccharomyces cerevisiae*.

In the next section, we solve Equation 10 numerically and analytically more generally.

3.3. Numerically solving the self-consistent equation

The self-consistent equation 10 can be numerically solved by iterating the following procedure. First, we start with initial guesses for the solutions $\psi_{\text{birth}}^{(0)}[\sigma_b]$ and $\Lambda_p^{(0)}$. We

then update our guess for the distribution $\psi_{\text{birth}}[\sigma_b]$ using Equation 10. Next, we update Λ_p by using the Euler-Lotka equation [12], obtained by integrating Equation 10 with respect to σ_b . This procedure is summarized in this set of equations:

$$\tilde{\psi}_{\text{birth}}^{(n)}[\sigma_b] = 2 \int f(\sigma_b | \sigma'_b, a') \psi_{\text{birth}}^{(n-1)}[\sigma'_b] g(a') e^{-\Lambda_p^{(n-1)} \tau[\sigma'_b]} da' d\sigma'_b, \quad (15)$$

$$\psi_{\text{birth}}^{(n)}[\sigma_b] = \frac{\tilde{\psi}_{\text{birth}}^{(n)}[\sigma_b]}{\int d\sigma'_b \tilde{\psi}_{\text{birth}}^{(n)}[\sigma'_b]} \quad (16)$$

$$1 = 2 \int \int \psi_{\text{birth}}^{(n)}[\sigma'_b] g(a') e^{-\Lambda_p^{(n)} \tau[\sigma'_b]} da' d\sigma'_b. \quad (17)$$

$\psi_{\text{birth}}^{(n)}$ and $\Lambda_p^{(n)}$ converge to constant values as $n \rightarrow \infty$. Note that the solution is not sensitive to the choice of $\psi_{\text{birth}}^{(0)}$ and $\Lambda_p^{(0)}$. In Figure 2, we compare the numerical solution for Equation 10 in the case of deterministic a (i.e. $g(a')$ is a delta function) and the fitted exponential growth rate obtained by simulating the population directly (see Appendix A for details of the simulation).

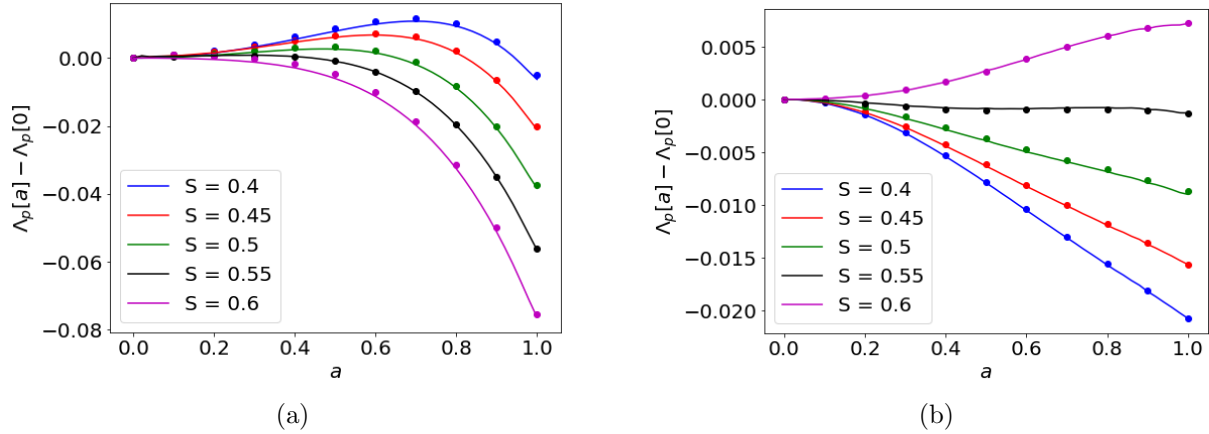


Figure 2: The relative population growth rate, compared to $a = 0$, is plotted against the asymmetry a . The solid lines show the numerical solutions of Equation 10 and the circles mark simulated population growth rates. (a) Beneficial protein ($\lambda_0 = 0.2, \lambda_1 = 1.2, n = 2$), (b) Deleterious protein ($\lambda_0 = 1, \lambda_1 = 0, n = 2$). For numerical solutions, we use $\psi_{\text{birth}}^{(0)}[\sigma] = \delta(\sigma_b - S)$ and $\Lambda_p^{(0)} = \ln 2 / \lambda[S]$. Error bars are smaller than the marker size.

Figure 2 confirms that Equation 10 has sufficient information for calculating the population growth rate. The iterative procedure is more accurate, faster, and less memory-intensive than a brute force simulation which involves exponentially growing population size. However, the main shortcoming of the numerical solution is that it does not give any insight about how Λ_p depends on S and a . It is possible infer the relation by finding Λ_p for various values of S and a , but for every parameter values, we have to go through Equations 15 - 17, which is highly inefficient. For those reasons, the

moment expansion method we discuss in the following section is a good alternative way of calculating Λ_p for small a .

3.4. Moment expansion

Equation 10 can be approximately solved by expanding the moments of $\psi_{\text{birth}}[\sigma_b]$. For simplicity, we start with the deterministic case. As we will explain in the following sections, it is straightforward to generalize this moment expansion method to the stochastic case.

When the key protein segregation is perfectly symmetric (i.e. $a = 0$), every cell has a concentration of key protein of $\sigma_b = S$ at cell birth. Therefore, for a small a , the distribution $\psi_{\text{birth}}[\sigma_b]$ should be sharply peaked around S . Based on this, we are motivated to expand the moment of the distribution around $\sigma_b = S$ by defining $\Delta\sigma_b = \sigma_b - S$. In order to calculate the n -th moment, we multiply both sides of Equation 10 by $\Delta\sigma_b^n$ and integrate them with respect to σ_b . We use Equations 8 and 9 to specify $f(\sigma_b|\sigma'_b, a')$ and $g(a')$. Invoking Newton's binomial theorem, we obtain:

$$\langle \Delta\sigma_b^n \rangle = \frac{1}{2^{n-1}} \sum_{m=0}^{\lfloor n/2 \rfloor} \binom{n}{2m} a^{2m} \langle \Delta\sigma_b^{n-2m} (\Delta\sigma_b + 2S)^{2m} e^{-\Lambda_p \tau[\Delta\sigma_b + S]} \rangle. \quad (18)$$

Note that by convention, $\binom{n}{0} = 1$. From the right hand side of Equation 18, we can infer that $\langle \Delta\sigma_b^n \rangle = O(a^{2\lfloor n/2 \rfloor})$. This means that by solving a system of $2k + 1$ equations ($n = 0, \dots, 2k$), we will find Λ_p to $O(a^{2k})$ accuracy. For each equation, we need to expand the exponential function $e^{-\Lambda_p \tau[\Delta\sigma_b + S]}$ around $\Delta\sigma_b = 0$ to order $a^{2\lfloor n/2 \rfloor}$. To illustrate the process more clearly, let us calculate Λ_p to $O(a^2)$ accuracy.

If $a = 0$, every cell has $\sigma_b = S$ when the population is stabilized, so $\Lambda_p = \frac{\ln 2}{\tau[S]}$. Due to symmetry, $\Lambda_p[a] = \Lambda_p[-a]$. Thus, to solve Λ_p to $O(a^2)$ is equivalent to finding a coefficient C_2 defined as below,

$$\Lambda_p = \frac{\ln 2}{\tau[S]} (1 + C_2 a^2 + O(a^4)). \quad (19)$$

Taylor expanding $\tau[\Delta\sigma_b + S]$ around $\Delta\sigma_b = 0$ to $O(a^2)$ we find

$$\tau[\Delta\sigma_b + S] = \tau[S] + \tau'[S] \Delta\sigma_b + \frac{\tau''[S]}{2} \Delta\sigma_b^2. \quad (20)$$

Expanding $e^{-\Lambda_p \tau[\Delta\sigma_b + S]}$ to $O(a^2)$ leads to:

$$e^{-\Lambda_p \tau[\Delta\sigma_b + S]} = \frac{1}{2} \left[1 - \ln 2 \left(C_2 a^2 + \frac{\tau'[S]}{\tau[S]} \Delta\sigma_b + \left(\frac{\tau''[S]}{2\tau[S]} - \frac{\ln 2}{2} \frac{\tau'[S]^2}{\tau[S]^2} \right) \Delta\sigma_b^2 \right) \right]. \quad (21)$$

Applying these to Equation 18 while setting $n = 0, 1$, or 2 , we can set up a system of three linear equations with the unknowns being C_2 , $\langle \Delta\sigma_b \rangle$ and $\langle \Delta\sigma_b^2 \rangle$. (Note that here $\tau[S]$ is a known function specified in the model.)

$$1 = 1 - \ln 2 \left[C_2 a^2 + \frac{\tau'[S]}{\tau[S]} \langle \Delta \sigma_b \rangle + \frac{\tau''[S]}{2\tau[S]} \langle \Delta \sigma_b^2 \rangle - \frac{\ln 2}{2} \frac{\tau'[S]^2}{\tau[S]^2} \langle \Delta \sigma_b^2 \rangle \right], \quad (22)$$

$$\langle \Delta \sigma_b \rangle = \frac{\langle \Delta \sigma_b \rangle}{2} - \frac{\ln 2}{2} \frac{\tau'[S]}{\tau[S]} \langle \Delta \sigma_b^2 \rangle, \quad (23)$$

$$\langle \Delta \sigma_b^2 \rangle = \frac{\langle \Delta \sigma_b^2 \rangle}{4} + S^2 a^2. \quad (24)$$

Solving these, we get

$$\langle \Delta \sigma_b \rangle = -\frac{4 \ln 2}{3} \frac{\tau'[S]}{\tau[S]} S^2 a^2, \quad (25)$$

$$\langle \Delta \sigma_b^2 \rangle = \frac{4}{3} S^2 a^2, \quad (26)$$

$$C_2 = -\frac{2}{3} \frac{\tau''[S]}{\tau[S]} S^2 + 2 \ln 2 \frac{\tau'[S]^2}{\tau^2[S]} S^2. \quad (27)$$

Therefore, the population growth rate is

$$\Lambda_p = \frac{\ln 2}{\tau[S]} \left(1 + \left(-\frac{2}{3} \frac{\tau''[S]}{\tau[S]} + 2 \ln 2 \frac{\tau'[S]^2}{\tau^2[S]} \right) S^2 a^2 \right). \quad (28)$$

This is general to any choice of $\tau[\sigma_b]$, but in particular, if the generation time is described by Equation 2, we can rewrite the population growth rate in terms of $\lambda[S]$.

$$\Lambda_p = \lambda[S] \left(1 + \frac{\lambda''[S]}{4 \ln 2 \lambda[S]} S^2 a^2 \right). \quad (29)$$

This second order solution for Λ_p is consistent with the result by *Lin et al.* [1] but is derived here more rigorously and more generally since it applies to any functional form of $\tau[\sigma_b]$. Furthermore, we can calculate Λ_p to an arbitrarily high order as desired by solving for $\Lambda_p = \frac{\ln 2}{\tau[S]} (1 + C_2 a^2 + C_4 a^4 + \dots)$, as we elaborate in Appendix C.

4. Phase transition of a_c

In this section, we investigate the phase transition of the optimal asymmetry a_c as a function of key protein accumulation rate S .

Previously, *Lin et al.* [1] inferred $a_c[S]$ by interpolating the solutions near $a = 0$ and at $a = 1$ with a minimal number of extrema. Due to the self-similarity in a population tree, they find a closed formula for $\Lambda_p[a = 1]$:

$$\sum_{i=0}^{\infty} \exp \left(-\Lambda_p[a = 1] \sum_{j=0}^i \tau[jS] \right) = 1. \quad (30)$$

The authors define S_* as the value S where $a = 0$ and $a = 1$ yield the same population growth rate. Near $a = 0$, *Lin et al.* study the dynamics of the total cell volume ($V = \sum_i v_i(t)$).

$$\frac{dV}{dt} = \sum_i \lambda[\sigma_{b,i}] v_i. \quad (31)$$

Then, they expand $\lambda[\sigma]$ around $\sigma = S$ and find that the second derivative of $\lambda[\sigma]$ determines whether $\Lambda_p[a]$ is an increasing or decreasing function near $a = 0$. This naturally leads to defining another critical value S_c where $\left. \frac{d^2\lambda}{d\sigma^2} \right|_{S=S_c} = 0$ defining the boundary between the regime where $a = 0$ is a local minimum to one where it is a local maximum. In the figure below, we summarize the graphical interpolation *Lin et al.* used to predict a sharp transition of a_c in the case of damage, and a smooth transition in the case of beneficial key proteins.

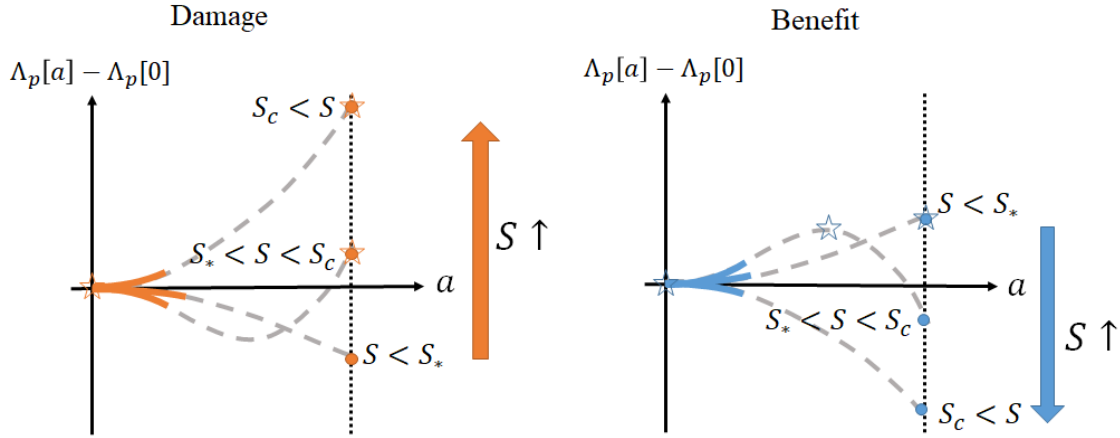


Figure 3: Finding the optimal asymmetry a_c by graphical interpolation [1]. *Lin et al.* find the second derivative of the fitness ($\Lambda_p[a] - \Lambda_p[0]$) near $a = 0$ (solid line) and numerically solve the self-consistent equation for $a = 1$ (Equation 30, filled circles). Interpolating between the two limits with a minimal number of extrema, the authors find what value of a maximizes the fitness (empty stars). Unlike in the damage case, in the benefit case, there is a large range of S where the fitness curve is convex near $a = 0$ and $\Lambda_p[a = 1] < \Lambda_p[a = 0]$ (i.e. $S_* < S < S_c$). This means that the population growth rate is maximized when a is between 0 and 1.

Similar to the previous paper by *Lin et al.*, we use an interpolation to infer where the phase transition of a_c is. In addition, we are equipped with a more rigorous way of finding the population growth rate near $a = 0$ as described in Section 3.4. We also have a transcendental equation about the slope of $\Lambda_p[a]$ at $a = 1$, which we discuss in depth in Appendix B. We denote the solution to Equation 30 as Λ_{p1} and expand $\Lambda_p[a] = \Lambda_{p1}(1 + C_1(1 - a) + O((1 - a)^2))$. Finding the sign of C_1 makes it possible to predict whether $\Lambda_p[a = 1]$ is a local minimum ($C_1 > 0$) or a local maximum ($C_1 < 0$). Using a similar moment expansion approach as we do for $a \approx 0$, we find the first coefficient C_1 in Appendix B as

$$C_1 = \frac{S \sum_{i=0}^{\infty} e^{-\Lambda_{p1} \sum_{j=0}^i \tau[jS]} \sum_{k=0}^i \tau'[kS] \left(\sum_{m=0}^{\infty} (m+1) e^{-\Lambda_p \sum_{n=0}^m \tau[nS]} - \frac{k(k+1)}{2} \right)}{2 \sum_{i=0}^{\infty} e^{-\Lambda_{p1} \sum_{j=0}^i \tau[jS]} \sum_{k=0}^i \tau[kS]} \quad (32)$$

Here we can define another critical value $S_c^{a=1}$ which is the value of S that makes

$C_1 = 0$. Because $\tau'[kS] > 0$ ($\tau'[kS] < 0$) for the damage (benefit) case, C_1 starts out positive (negative) for a small S and becomes negative (positive) as S exceeds $S_c^{a=1}$. In other words, when $S < S_c^{a=1}$, $a = 1$ is a local minimum (maximum) of $\Lambda_p[a]$, whereas it becomes a local maximum (minimum) when $S > S_c^{a=1}$ in the damage (benefit) case. This provides us an additional piece of information that we can use to infer whether $a_c = 1$ for a given S . For instance, in the case of damage ($\lambda_0 = 1, \lambda_1 = 0$), $S_c^{a=1} \approx 0.592$ is greater than $S_* \approx 0.558$. This means that if S is between S_* and $S_c^{a=1}$, $\Lambda_p[a]$ should have a local maximum below $a = 1$. When S is above both S_* and $S_c^{a=1}$, the population growth rate is maximized at $a = 1$ (i.e. $a_c = 1$). This means that the transition of a_c is not a single discrete jump from $a_c = 0$ to $a_c = 1$, but rather a jump to an intermediate $a_c \in (0, 1)$ and then a smooth increase to $a_c = 1$. This process is illustrated in Figure 4.

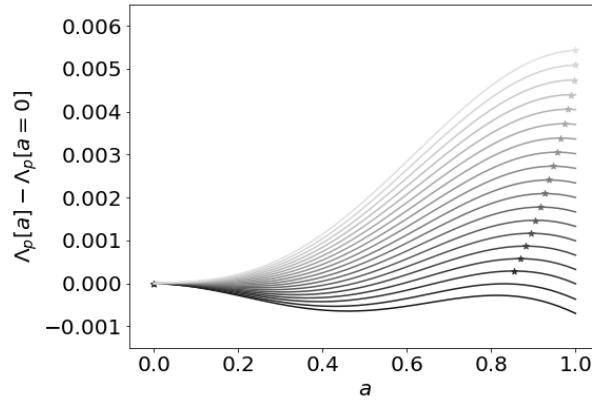


Figure 4: Increase of Λ_p relative to $a = 0$ against a_c calculated by numerically solving Equation 10. S increases as the line gets lighter ($S = 0.554$ to 0.592). The stars mark a_c for each S . If $S < S_*$, then automatically, $S < S_c$ and $S < S_c^{a=1}$. This means that $a = 0$ is a local maximum and there is also another peak between $a = 0$ and $a = 1$. At $S = S_*$, $S < S_c^{a=1}$, which means that there is $a < 1$ that has a higher Λ_p than $a = 0$ and $a = 1$. Therefore, there should be a first-order phase transition at $S < S_*$.

In the case of beneficial key proteins, *Lin et al.* found that $a_c = 1$ for small S and decreases smoothly to $a_c = 0$ as S increases, but the start of that transition was not specified. Based on Appendix B, we find that a_c starts deviating from one at $S_c^{a=1} = 0.214$ (blue dotted line in Figure 5 (a)), consistent with the numerical solution of Equation 10. Comparing the solid blue line (a_c predicted by the moment expansion to the sixth order) and the orange dots (numerical simulation), note that the moment expansion method does not successfully predict a_c when the true a_c value is close to 1. However, as S increases, and a_c becomes closer to 0, the answers agree better, since $a^2 \approx 0$ our approximation holds.

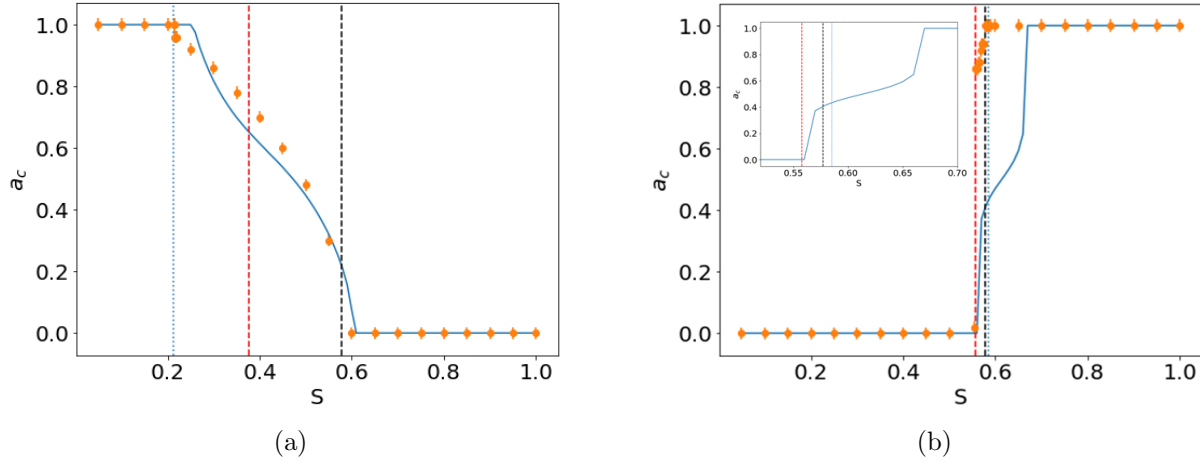


Figure 5: a_c , the value of a that maximizes the population growth rate, plotted against S . The solid blue lines are the prediction made from the sixth order solution of Λ_p . The orange points, each of which has an error bar, show a_c found by solving Equation 10 numerically as described in section 3.3. (a) Beneficial protein ($\lambda_0 = 0.2, \lambda_1 = 1.2, n = 2$), (b) Deleterious protein ($\lambda_0 = 1, \lambda_1 = 0, n = 2$). The inset zooms in on the region around $S = 0.6$. The dotted blue line shows where the slope of Λ_p at $a = 1$ changes its sign. The red dashed line is at $S = S_*$ where $\Lambda_p[a = 0] = \Lambda_p[a = 1]$ and the black dashed line is at $S = S_c$ where $\lambda''[S] = 0$ (i.e. the second derivative of $\Lambda_p[a]$ changes its sign at $a = 0$).

5. Introducing noise

The moment expansion method can be easily generalized to the stochastic model where a is drawn from a distribution $g(a)$ every time a cell divides. Equation 18 becomes

$$\langle \Delta \sigma_b^n \rangle = \frac{1}{2^{n-1}} \sum_{m=0}^{\lfloor n/2 \rfloor} \binom{n}{2m} \int g(a) a^{2m} da \langle \Delta \sigma_b^{n-2m} (\Delta \sigma_b + 2S)^{2m} e^{-\Lambda_p \tau [\Delta \sigma_b + S]} \rangle. \quad (33)$$

This implies that in the small a limit, we can define an effective a , $a_{\text{eff}} = \sqrt{\langle a^2 \rangle}$, for which the population growth rate Λ_p has the same formula independent of $g(a)$.

$$\Lambda_p = \lambda[S] \left(1 + \frac{\lambda''[S]}{4 \ln 2 \lambda[S]} S^2 a_{\text{eff}}^2 \right). \quad (34)$$

In Figure 6, we numerically solve Equation 10 where $g(a)$ is a uniform distribution ($g(a) = U(\bar{a} - \sigma_a, \bar{a} + \sigma_b)$ with $\bar{a} = 0$ and $\sigma_a = 0, 0.1, 0.2, \dots, 1$) and plot the population growth rate against $a_{\text{eff}} = \sqrt{\langle a^2 \rangle}$. As predicted, a_{eff} behaves exactly as a does in the deterministic model for a broad range of σ_a . For a relatively large S and large σ_a , the population growth rate obtained by simulating the exponentially growing population starts to deviate from the second order prediction as shown in Figure 6. This conclusion that stochastic segregation of key proteins increases effective asymmetry is analogous to the finding made by *Chao et al.* [11] about damage partitioning in *E. coli* that larger

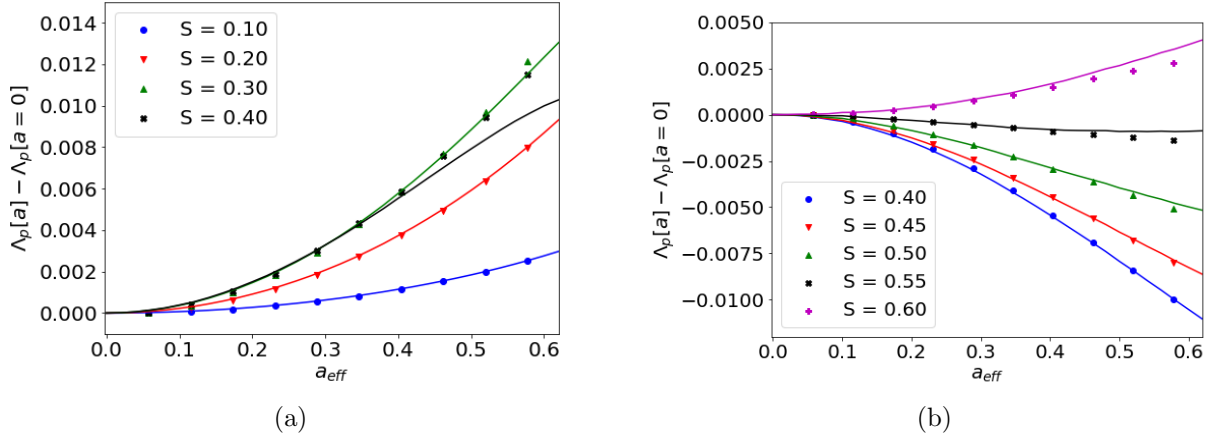


Figure 6: The change of population growth rate ($\Lambda_p[a_{\text{eff}}] - \Lambda_p[a = 0]$) plotted against the effective value of a where $g(a) = U(\bar{a} - \sigma_a, \bar{a} + \sigma_a)$, a uniform distribution. The solid lines show the numerical solutions of Equation 10 for $\sigma_a = 0$ and the circles correspond to simulated values where $\bar{a} = 0$ and $\sigma_a = 0, 0.1, 0.2, \dots, 1$. (a) Beneficial protein ($\lambda_0 = 0.2, \lambda_1 = 1.2, n = 2$), (b) Deleterious protein ($\lambda_0 = 1, \lambda_1 = 0, n = 2$).

fluctuations result in similar increase of the population growth as a fixed asymmetric ratio.

6. Asymmetry a as a variable of concentration of key proteins

So far, we have considered a model where the segregation ratio of key proteins is independent from the amount of key proteins each cell has. However, there is experimental evidence that the degree of asymmetry may depend on how much key proteins a cell has [3, 8]. *Vedel et al.* [6] studied how protein aggregates in *E. coli* created in responds to heatshock are segregated differently between two daughters. One of their results is that the asymmetric segregation parameter a is a function of the amount of protein aggregates D , and if a is assumed to be constant, the fitness is underestimated. We can test the effect of dependence of a to D by replacing a with $a[D]$ in Equation 10.

$$\psi_{\text{birth}}[\sigma_b] = 2 \int \psi_{\text{birth}}[\sigma'_b] f(\sigma_b | \sigma'_b, a[\sigma'_b + S]) e^{-\Lambda_p \tau [\sigma'_b]} d\sigma'_b. \quad (35)$$

Here we replaced D with $\sigma'_b + S$ since we assume the cell volume always is 1 at birth and 2 at division. In Figure 7, we show the numerical value of population growth rate increase due to asymmetry ($\Lambda_p[a] - \Lambda_p[a = 0]$), while a is a function of the amount of protein at division. Specifically, we set $a[D] = \tanh(kD)$ and tune k . In other words, we assume a to increase from zero initially with the slope k and asymptotically approach $a = 1$. Qualitatively, we expect the effective a to be small when S is small, and it becomes closer to 1 as S gets larger. We can check this intuition by writing down the equation for the moments of ψ_{birth} analogous to Equation 18.

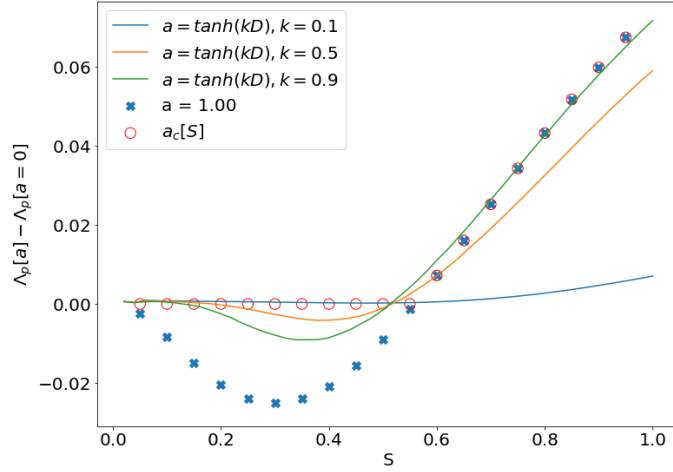


Figure 7: The change of population growth rate ($\Lambda_p[a = \tanh(kD)] - \Lambda_p[a = 0]$) plotted against accumulation rate S . Here the key proteins are deleterious ($\lambda_0 = 1, \lambda_1 = 0, n = 2$). The blue cross show the values when a is fixed at 1 ($\Lambda_p[a = 1] - \Lambda_p[a = 0]$) and the red circles show the change of the population growth rate when a is equal to the optimal value a_c at a given S .

$$\langle \Delta\sigma_b^n \rangle = \frac{1}{2^{n-1}} \sum_{m=0}^{\lfloor n/2 \rfloor} \binom{n}{2m} \langle a[\Delta\sigma_b + 2S]^{2m} \Delta\sigma_b^{n-2m} (\Delta\sigma_b + 2S)^{2m} e^{-\Lambda_p \tau [\Delta\sigma_b + S]} \rangle. \quad (36)$$

If the slope of $a[D]$ is small compared to a^2 , we can approximate $a[\Delta\sigma_b + 2S]^{2m} \approx a[2S]$. Note that the population growth rate can be higher with an adaptive a (e.g. with $k = 0.9, 0.55 < S < 0.65$) than when a is fixed at $a_c[S]$ (orange dots in Figure 7). Qualitatively, this suggests that there is an advantage if each cell tunes the asymmetry of segregation according to its level of damage.

7. Discussion and outlook

In this paper, we investigate how asymmetric segregation of key proteins in microbial organisms impact the population growth rate with a self-consistent equation (Equation 10) solved analytically and numerically. We adapt a physiological model proposed by *Lin et al.* [1] and apply the transport equation to set up an equation for the distribution of protein concentration at birth $\psi[\sigma_b]$ and population growth rate Λ_p (Equation 10). The equation can be solved by updating the solutions iteratively as elaborated in Section 3.3. When the asymmetry is small ($a \ll 1$), Λ_p can be approximated to a^{2n} precision by solving a set of linear equations with respect to the moments of $\psi[\sigma_b]$ and Λ_p . Similar approximations can be made from the opposite limit, $a \approx 1$ (see Appendix B). Changing the accumulation rate of key proteins, S , we confirm the sharp phase transition of a_c for a deleterious protein and a smooth transition for a beneficial protein as *Lin et al.* reported [1]. In addition, since numerically solving Equation 10 provides more precise prediction of Λ_p than a direct simulation of an exponentially growing population, we are

able to find that the phase transition in the case of damage is composed of a discrete jump to a_c between 0 and 1 and a smooth increase to $a_c = 1$. We also explore different physiological models motivated by experimental studies. We discuss the case where the cell tunes the asymmetry with response to the amount of key proteins it has at division and how the adaptive strategy may minimize the disadvantage of asymmetry when the accumulation rate of damage is low. Finally, we show by generalizing our model that even if the segregation ratio is on average symmetric, the noise can have a similar effect as an asymmetric segregation.

There are many other aspects of asymmetric division in biology where our theoretical framework might be useful for building a theoretical model [2, 15]. First, there are many other ways that microbes develop phenotypic diversity rather than due to asymmetric key protein segregation. For instance, budding yeast (*Saccharomyces cerevisiae*) has cell size difference between a daughter (smaller cell) and mother cell (bigger cell), whereas when a *Caulobacter crescentus* cell divides, one is non-motile and reproductive and the other swarms and does not divide until maturation [16, 17]. In the former case, introduction of volume asymmetry turns out to create interesting correlations between the noise in growth and the population growth rate [18]. Second, mortality rate rather than volumetric growth rate may depend on the key protein concentration [19]. Lastly, connecting back to multicellular organisms, where the theory of aging (soma theory) was first proposed [20], can be interesting both mathematically and biologically. Major difference from microbial system is that the cells interact with the neighbors and use the cues to make decisions [21]. Considering the geometry of the tissue might complicate the model beyond the level of a self-consistent equation can capture, but plants which have rigid tissue and simpler geometry may be a good starting point for a theoretical investigation [22].

8. Acknowledgements and Funding Sources

The authors thank the Amir group, the Desai lab, Andrew Murray, Jane Kondev and Doeke Hekstra for helpful discussions. J. M. acknowledges Yubo Su for helping improve numerical simulations. A. A. was supported by the NSF CAREER award number 1752024.

Appendix A. Simulation details

When we explicitly simulate the exponentially growing population, we start with 100 cells with uniform distribution of age. We run until the number of cells reaches 5×10^6 and find the slope of $\ln(\sum V(t))$ after $t = 5$. This use of sum of volume rather than the number of cells for finding the population growth rate is because the volume increases continuously and the growth rate should be equivalent if the cell size is controlled. Python scripts for the simulations are on our Github.

Appendix B. Λ_p when $a \approx 1$

The challenge for a highly asymmetric case is that the distribution $\psi_{\text{birth}}[\sigma_b]$ is not symmetric around S . Because one of two newborn cells is rejuvenated at each division, we would expect the distribution to be skewed to the right and maximized near $\sigma_b = 0$. This means that we should expand $\psi_{\text{birth}}[\sigma_b]$ around different values depending on when the cell has been rejuvenated for the last time (i.e. generational age), in order to solve the self-consistent equation. Categorizing cells based on their generational age, we can rewrite the self-consistent equation (10) as,

$$\begin{aligned}\psi_0[\sigma_b] &= \int \sum_{i=0}^{\infty} \psi_i[\sigma'_b] f(\sigma_b, R|\sigma'_b) e^{-\Lambda_p \tau[\sigma'_b]} d\sigma'_b, \\ \psi_i[\sigma_b] &= \int \psi_{i-1}[\sigma'_b] f(\sigma_b, S|\sigma'_b) e^{-\Lambda_p \tau[\sigma'_b]} d\sigma'_b (i > 0).\end{aligned}\tag{B.1}$$

Here $\psi_i[\sigma_b]$ is the probability that a cell has protein concentration σ_b at birth and the pole age i . The transition function for the rejuvenated cell is $f(\sigma, R|\sigma'_b) = \delta\left(\sigma - \frac{1-a}{2}(\sigma'_b + S)\right)$, and the senescent is $f(\sigma, S|\sigma'_b) = \delta\left(\sigma - \frac{1+a}{2}(\sigma'_b + S)\right)$. Note that the rejuvenating transition function does not depend on σ'_b (parent cell) if $a = 1$. This is equivalent to the property used by Lin et al. [1] to find a closed formula for $\Lambda_p[a = 1]$: there is a self-symmetry in a population tree in a stable exponential growth.

$$1 = \sum_{i=0}^{\infty} \exp\left[-\sum_{j=0}^i \Lambda_p \tau[jS]\right].\tag{B.2}$$

Here, we can use the fact that every $\psi_i[\sigma_b]$ is a delta function if $a = 1$.

$$\begin{aligned}\psi_i[\sigma_b] &= \int \psi_{i-1}[\sigma'_b] \delta(\sigma_b - (\sigma'_b + S)) e^{-\Lambda_p \tau[\sigma'_b]} d\sigma'_b \\ &= \psi_{i-1}[\sigma_b - S] e^{-\Lambda_p \tau[\sigma_b - S]} \\ &= \psi_0[\sigma_b - iS] e^{-\sum_{j=1}^i \Lambda_p \tau[\sigma_b - jS]} (i > 0)\end{aligned}\tag{B.3}$$

$$\begin{aligned}\psi_0[\sigma_b] &= \int \sum_{i=0}^{\infty} \psi_i[\sigma'_b] \delta(\sigma_b) e^{-\Lambda_p \tau[\sigma'_b]} d\sigma'_b \\ &= \delta(\sigma_b) \int \sum_{i=0}^{\infty} \psi_0[\sigma_b - iS] \exp\left[-\sum_{j=0}^i \Lambda_p \tau[\sigma_b - jS]\right] d\sigma'_b\end{aligned}\tag{B.4}$$

By integrating $\psi_0[\sigma_b]$ with respect to σ_b , we get

$$1 = \sum_{i=0}^{\infty} \exp\left[-\sum_{j=0}^i \Lambda_p \tau[(i-j)S]\right] = \sum_{i=0}^{\infty} \exp\left[-\sum_{j=0}^i \Lambda_p \tau[jS]\right],\tag{B.5}$$

which is consistent to the previous paper [1]. Let's call the unique solution for Equation B.5, $\Lambda_{p,1}$. Near $a = 1$, we can find the approximate population growth rate by expanding $\Lambda_p = \Lambda_{p,1}(1 + C_1(1-a) + C_2(1-a)^2 + \dots)$ where $a < 1$. As a deviates from 1, we expect each delta function to broaden near $\sigma_b = iS$. Similar to the case of

a small a , we will find the moments of $\psi_i[\sigma_b]$ starting from the lowest order. Here we will investigate the first order coefficient C_1 . Importantly, finding the sign of C_1 will allow us to predict whether $\Lambda_p[a = 1]$ is a local minimum ($C_1 > 0$) or a local maximum ($C_1 < 0$).

Let us define $\delta a = 1 - a$. To find C_1 we need to solve Equation B.1 to $O(\delta a)$. Thus, we can rewrite the equations as

$$\begin{aligned}\psi_0[\sigma_b] &= \int \sum_{i=0}^{\infty} \psi_i[\sigma'_b] \delta \left(\sigma_b - \frac{\delta a}{2} (\sigma'_b + S) \right) \\ &\quad \exp \left[-\Lambda_{p1} \tau[iS] (1 + C_1 \delta a) \left(1 + \frac{\tau'[iS]}{\tau[iS]} (\sigma'_b - iS) \right) \right] d\sigma'_b \\ \psi_i[\sigma_b] &= \int \psi_{i-1}[\sigma'_b] \delta (\sigma_b - (1 - \delta a/2)(\sigma'_b + S)) \\ &\quad \exp \left[-\Lambda_{p1} \tau[(i-1)S] (1 + C_1 \delta a) \right. \\ &\quad \left. \left(1 + \frac{\tau'[(i-1)S]}{\tau[(i-1)S]} (\sigma'_b - (i-1)S) \right) \right] d\sigma_b\end{aligned}\tag{B.6}$$

For brevity, from now on, we shall write $\Psi_i = \int \psi_i[\sigma_b] d\sigma_b$ and $\langle F[\delta\sigma_b] \rangle_i = \int \psi_i[\sigma_b] F[\sigma_b - iS] d\sigma_b / \Psi_i$. First, let us integrate the i th equation ($i > 0$),

$$\begin{aligned}\Psi_i &= \int \psi_{i-1}[\sigma'_b] e^{-\Lambda_{p1} \tau[\sigma'_b]} d\sigma'_b \\ &= e^{-\Lambda_{p1} \tau[(i-1)S]} \int \psi_{i-1}[\sigma'_b] \\ &\quad (1 - \Lambda_{p1} \tau[(i-1)S] C_1 \delta a - \Lambda_{p1} \tau'[(i-1)S] (\sigma'_b - (i-1)S)) d\sigma'_b \\ &= \Psi_{i-1} e^{-\Lambda_{p1} \tau[(i-1)S]} \left(1 - \Lambda_{p1} \tau[(i-1)S] C_1 \delta a - \langle \delta\sigma_b \rangle_{i-1} \Lambda_{p1} \tau'[(i-1)S] \right) \\ &= \Psi_0 e^{-\Lambda_{p1} \sum_{j=0}^{i-1} \tau[jS]} \left(1 - \Lambda_{p1} \sum_{k=0}^{i-1} \tau[kS] C_1 \delta a - \langle \delta\sigma_b \rangle_k \Lambda_{p1} \tau'[kS] \right) + O(\delta a^2)\end{aligned}\tag{B.7}$$

For $i = 0$ we have

$$\begin{aligned}\Psi_0 &= \sum_{i=0}^{\infty} \int \psi_i[\sigma'_b] e^{-\Lambda_{p1} \tau[\sigma'_b]} d\sigma'_b \\ &= \sum_{i=1}^{\infty} \Psi_i \\ &= \Psi_0 \sum_{i=0}^{\infty} e^{-\Lambda_{p1} \sum_{j=0}^i \tau[jS]} \left(1 - \Lambda_{p1} \sum_{k=0}^i \tau[kS] C_1 \delta a - \langle \delta\sigma_b \rangle_k \Lambda_{p1} \tau'[kS] \right),\end{aligned}\tag{B.8}$$

to $O(\delta a)$ accuracy. Using the definition of $\Lambda_{p1} - 1 = \sum_{i=0}^{\infty} e^{-\Lambda_{p1} \sum_{j=0}^i \tau[jS]}$, we can extract an expression for the coefficient C_1 .

$$\begin{aligned}C_1 &= - \frac{\sum_{i=0}^{\infty} e^{-\Lambda_{p1} \sum_{j=0}^i \tau[jS]} \sum_{k=0}^i \tau'[kS] \langle \delta\sigma_b \rangle_k}{\sum_{i=0}^{\infty} e^{-\Lambda_{p1} \sum_{j=0}^i \tau[jS]} \sum_{k=0}^i \tau[kS] \delta a} \\ &= - \frac{\sum_{k=0}^{\infty} \tau'[kS] \langle \delta\sigma_b \rangle_k \sum_{i=k}^{\infty} e^{-\Lambda_{p1} \sum_{j=0}^i \tau[jS]}}{\delta a \sum_{k=0}^{\infty} \tau[kS] \sum_{i=k}^{\infty} e^{-\Lambda_{p1} \sum_{j=0}^i \tau[jS]}}\end{aligned}\tag{B.9}$$

Let us find $\langle \delta\sigma_b \rangle_i$ for $i > 0$.

$$\begin{aligned}
\langle \sigma_b \rangle_i &= \frac{1}{\Psi_i} e^{-\Lambda_{p1} \tau[(i-1)S]} \int \psi_{i-1}[\sigma'_b] \\
&\left(\left(1 - \frac{\delta a}{2} \right) (\sigma'_b - (i-1)S + iS) - iS \right) \\
&(1 - \Lambda_{p1} \tau[(i-1)S] C_1 \delta a - \Lambda_{p1} \tau'[(i-1)S] (\sigma'_b - (i-1)S)) d\sigma'_b \\
&= -\frac{\delta a}{2} iS + \frac{1}{\Psi_i} e^{-\Lambda_{p1} \tau[(i-1)S]} \Psi_{i-1} \langle \delta \sigma_b \rangle_{i-1} \\
&= -\frac{\delta a}{2} \sum_{k=0}^i (i-k) S \frac{\Psi_{i-k}}{\Psi_i} e^{-\Lambda_{p1} \sum_{j=1}^k \tau[(i-j)]} \\
&+ \frac{\Psi_0}{\Psi_i} e^{-\Lambda_{p1} \sum_{j=0}^{i-1} \tau[jS]} \langle \delta \sigma_b \rangle_0 \\
&= -\delta a \frac{S i(i+1)}{2} + \langle \delta \sigma_b \rangle_0 + O(\delta a^2)
\end{aligned} \tag{B.10}$$

If $i = 0$,

$$\begin{aligned}
\langle \delta \sigma_b \rangle_0 &= \frac{1}{\Psi_0} \frac{\delta a}{2} \sum_{m=0}^{\infty} \psi_m[\sigma'_b] (\sigma'_b - mS + (m+1)S) \\
&[1 - \Lambda_{p1} \tau[mS] C_1 \delta a - \Lambda_{p1} \tau'[mS] (\sigma'_b - mS)] d\sigma'_b \\
&= \frac{1}{\Psi_0} \frac{\delta a}{2} \sum_{m=0}^{\infty} (m+1) S \Psi_{m+1}
\end{aligned} \tag{B.11}$$

$$= \frac{\delta a}{2} \sum_{m=0}^{\infty} (m+1) S e^{-\Lambda_{p1} \sum_{n=0}^m \tau[nS]} + O(\delta a^2) \tag{B.12}$$

This shows that $\langle \delta \sigma_b \rangle_i$ is positive for small i and becomes more and more negative as i increases. Applying this to Equation B.9, we can find the slope near $a = 1$.

$$C_1 = \frac{S \sum_{i=0}^{\infty} e^{-\Lambda_{p1} \sum_{j=0}^i \tau[jS]} \sum_{k=0}^i \tau'[kS] \left(-\frac{k(k+1)}{2} + \sum_{m=0}^{\infty} (m+1) e^{-\Lambda_{p1} \sum_{n=0}^m \tau[nS]} \right)}{\sum_{i=0}^{\infty} e^{-\Lambda_{p1} \sum_{j=0}^i \tau[jS]} \sum_{k=0}^i \tau[kS]} \tag{B.13}$$

Appendix C. Finding $\Lambda_p[a]$ to $O(a^{2n})$ ($n > 1$)

In order to calculate $\Lambda_p[a]$ to $O(a^{2n})$ accuracy, we write Λ_p and $\tau[\sigma_b]$ as

$$\Lambda_p = \frac{\ln 2}{\tau[S]} \left(1 + \sum_{k=1}^n C_{2k} a^{2k} \right), \tag{C.1}$$

$$\tau[\sigma'_b] = \tau[S] \sum_{i=0}^{2n} \frac{\tau^{(i)}[S]}{i! \tau[S]} \Delta \sigma_b^i. \tag{C.2}$$

Using these, we write

$$e^{-\Lambda_p \tau[\sigma_b]} = \exp \left[-\ln 2 \left(1 + \sum_{k=1}^n C_{2k} a^{2k} \right) \sum_{i=0}^{2n} \frac{\tau^{(i)}[S]}{i! \tau[S]} \Delta \sigma_b^i \right]. \tag{C.3}$$

Next, we should expand Equation 18 and truncate any terms with higher order than a^{2n} . We can also rewrite $\langle \sigma_b^m \rangle$ ($1 \leq m \leq 2n$) as

$$\langle \Delta \sigma_b^{2k} \rangle = \sum_{j=k}^n D_{2k}^{(2j)} a^{2j}, \quad (\text{C.4})$$

$$\langle \Delta \sigma_b^{2k-1} \rangle = \sum_{j=k}^n D_{2k+1}^{(2j)} a^{2j}. \quad (\text{C.5})$$

Maintaining only terms to $O(a^{2n})$ and matching the coefficients of a^{2j} ($1 \leq j \leq n$), we can solve the system of equations for D and C 's. We provide the SymPy code to find the coefficients on our Github repository.

References

- [1] Lin J, Min J and Amir A 2019 *Physical Review Letters* **122** 068101
- [2] Levien E, Min J, Kondev J and Amir A 2020 *arXiv preprint arXiv:2010.05672*
- [3] Coelho M, Dereli A, Haese A, Kühn S, Malinowska L, DeSantis M E, Shorter J, Alberti S, Gross T and Tolić-Nørrelykke I M 2013 *Current Biology* **23** 1844–1852
- [4] Coelho M and Tolić I M 2015 *BioEssays* **37** 740–747
- [5] Vaubourgeix J, Lin G, Dhar N, Chenouard N, Jiang X, Botella H, Lupoli T, Mariani O, Yang G, Ouerfelli O *et al.* 2015 *Cell Host & Microbe* **17** 178–190
- [6] Vedel S, Nunns H, Košmrlj A, Semsey S and Trusina A 2016 *Cell Systems* **3** 187–198
- [7] Lindner A B, Madden R, Demarez A, Stewart E J and Taddei F 2008 *Proceedings of the National Academy of Sciences* **105** 3076–3081
- [8] Stewart E J, Madden R, Paul G and Taddei F 2005 *PLoS Biology* **3** e45
- [9] Ackermann M, Chao L, Bergstrom C T and Doebeli M 2007 *Aging Cell* **6** 235–244
- [10] Chao L 2010 *PLoS Genetics* **6** e1001076
- [11] Chao L, Rang C U, Proenca A M and Chao J U 2016 *PLoS Computational Biology* **12** e1004700
- [12] Levien E, Kondev J and Amir A 2020 *Journal of the Royal Society Interface* **17** 20190827
- [13] Blitvić N and Fernandez V I 2020 *Journal of Theoretical Biology* 110331
- [14] Hartwell L H and Unger M W 1977 *The Journal of Cell Biology* **75** 422–435
- [15] Moger-Reischer R Z and Lennon J T 2019 *Nature Reviews Microbiology* **17** 679–690
- [16] Curtis P D and Brun Y V 2010 *Microbiology and Molecular Biology Reviews* **74** 13–41
- [17] Obuchowski P L and Jacobs-Wagner C 2008 *Journal of Bacteriology* **190** 1718–1729
- [18] Barber F, Min J, Murray A W and Amir A 2020 *bioRxiv (Preprint 404012)*
- [19] Maisonneuve E, Ezraty B and Dukan S 2008 *Journal of Bacteriology* **190** 6070–6075
- [20] Kirkwood T B 1977 *Nature* **270** 301–304

- [21] Moore D L and Jessberger S 2017 *Trends in Cell Biology* **27** 82–92
- [22] Pillitteri L J, Guo X and Dong J 2016 *Cellular and Molecular Life Sciences* **73** 4213–4229